

Journal Pre-proof

Virtual Screening and Pharmacokinetics Analysis of Inhibitors against Tuberculosis: Structure and Ligand-Based Approach



Stephen E. Abechi , Abatyough Terungwa Michael ,
Ajala Abduljelil , Egeh Stephen , Otaru Habiba Asipita ,
Mohamed El Fadili

PII: S2468-2276(24)00029-2
DOI: <https://doi.org/10.1016/j.sciaf.2024.e02085>
Reference: SCIAF 2085

To appear in: *Scientific African*

Received date: 10 August 2023
Revised date: 22 December 2023
Accepted date: 9 January 2024

Please cite this article as: Stephen E. Abechi , Abatyough Terungwa Michael , Ajala Abduljelil , Egeh Stephen , Otaru Habiba Asipita , Mohamed El Fadili , Virtual Screening and Pharmacokinetics Analysis of Inhibitors against Tuberculosis: Structure and Ligand-Based Approach, *Scientific African* (2024), doi: <https://doi.org/10.1016/j.sciaf.2024.e02085>

This is a PDF file of an article that has undergone enhancements after acceptance, such as the addition of a cover page and metadata, and formatting for readability, but it is not yet the definitive version of record. This version will undergo additional copyediting, typesetting and review before it is published in its final form, but we are providing this version to give early visibility of the article. Please note that, during the production process, errors may be discovered which could affect the content, and all legal disclaimers that apply to the journal pertain.

© 2024 Published by Elsevier B.V.
This is an open access article under the CC BY-NC-ND license
(<http://creativecommons.org/licenses/by-nc-nd/4.0/>)

Virtual Screening and Pharmacokinetics Analysis of Inhibitors against Tuberculosis: Structure and Ligand-Based Approach

¹Stephen E. Abechi, ²Abatyough Terungwa Michael, ^{1*}Ajala Abduljelil, ¹Ejeh Stephen, ³Otaru Habiba Asipita, and ⁴Mohamed El Fadili

¹Chemistry Department, Ahmadu Bello University, Zaria, Nigeria

²Chemical Sciences department, Bingham University, Karu Nigeria

³Faculty of Physical Science, Department of Chemistry, Nigerian Defence Academy Kaduna

⁴LIMAS Laboratory, Faculty of Sciences Dhar El Mehraz, Sidi Mohammed Ben Abdellah University, BP 1796 Atlas, Fez 30000, Morocco

*Corresponding author: Chemistry Department Ahmadu Bello University, Zaria, Kaduna State 810107, Nigeria. E-mails: aajala@abu.edu.ng, ORCID ID: <http://orcid.org/0000-0002-9823-8847>, Tel: +2348039183847

Abstract

Life-threatening diseases like tuberculosis have raised concerns in the medical and scientific communities. The damage-causing disease makes the scientific community employ the *in-silico* approach for design of new inhibitors that can inhibit or retard the havoc caused by this deadly disease. The *insilico* approach was used in this study to create a mathematical model with promising molecular properties, and receptors from the library were used to screen compounds and estimate the kinetic ability of the screened inhibitors that can cure this disease. 2D molecular properties evolved in the built model with high predictive ability. Three inhibitors x, y, and z emerged with better and higher molecular properties, the lowest binding energy (and higher binding affinity), and a better pharmacokinetic assessment compared to the template used in designing the effective compounds, with binding affinities of -15.56 kcal/mol, -18.51 kcal/mol, and -18.58 kcal/mol, respectively. Virtual screening of these compounds showed that they have good binding energy and excellent docking positions with the inhibiting potential of the receptor.

Also, pharmacokinetic predictions and ADMET, depict orally active ability of the inhibitors, possess good human intestinal absorption, and violate none of the RO5 as potential drug candidates to cure this disease. Hence, further laboratory tests are recommended for these to determine their toxicities and biological assays.

Keywords: Rational design, Molecular properties, ADMET, Docking, QSAR

Introduction

An incurable, deadly disease called tuberculosis (TB) has been known for causing havoc and leading to a high death rate in society. In the world's population, TB affects above 2%; as such, perpetual research is allowed every now and then. Meanwhile, about two million people died as a result of TB between 2019 and 2020. According to records, about 15 million people worldwide are reportedly ill as an outcome of this contagious disease [1]. Lungs are the main target of this growing human disease [2]. Little or no appetite, weight loss, fever, and coughing are among the signs associated with this disease.

TB has developed resistance to several medicines, among them isoniazid rifampicin, and ethambutol, all of which are related to the transformation of genes. Most of the drugs are toxic and have side effects, which invariably contribute to the challenges caused by this disease. Also, inherent in this disease is hepatitis, which is another life-threatening disease in the world [3, 5]. To combat the atrocities caused by this disease, drugs have been produced using outdated methods that are inefficient and costly. Searching for methods that are cost-effective and less expensive with little or no side effects remains an area where medicinal scientists are investing efforts in finding effective TB agents against *M. tuberculosis* [6, 7].

Heterocyclic triazole and its derivatives possessed inherent properties with the ability to hinder or cure this disease, especially when the structures were related to the biological activities of the structures [3, 6, 9]. These bioactive chemical compounds have therapeutic ability embedded in their structures, which can be very instrumental in rational drug design [6, 10]. These triazoles possessed other ill-ness abilities such as malarial, tuberculosis, analgesic, and were very efficacious with anti-TBS activity [4–14].

Computational-Aided Drug Design (CADD) has been very instrumental in the research community and is known for its ability to yield positive results, especially in *in silico* drug design. The *in-silico* methods embedded in computational drug design approaches reduce the cost of drug design and analysis before production and further clinical testing [3]. Investigation and exploration of potential inhibitors carried out under simulation techniques, after successful application, normally give good results. Additionally, computational methods have been very useful tools in the exploitation of potential therapeutic oxadiazole inhibitors [3, 15, 16].

To design hypothetical compounds with great therapeutic ability that can cure or inhibit the atrocity caused by tuberculosis, a promising method is germane in order to successfully meet-up with the preparation and design of compounds with better activity. A lead compound emerged after interactions of experimental compounds with a protein target of interest; the compound with the smallest negative docking value was chosen as a template and lead compound to design several hypothetical compounds; this landmark was achieved with the aid of bioinformatics approaches and yielded excellent results [17, 18]. Some of the computational drug design methods used to create drugs with high potency and low toxicity are QSAR (Quantitative Structure-Activity Relationship) techniques and toxicity predictions [3].

Some factors have been responsible for the failure of most drugs at the clinical stages, such as absorption ability and insidious and bad kinetic potential. The ADMET method have recorded successful in forecasting these clinical failure factors. *In-silico* methods have been reported and are known for their ability to predict potential drug candidates in the human living system by employing modeling and simulation techniques. This alternative method has proven over the years to be outstanding, stand the test of time, and be cost- and time-effective, possess the ability to screen millions of compounds within a short time and rarely experience clinical failure when the methods are properly applied. Hence, this research aimed at utilizing an *in-silico* method to build a model with highly predictive ability using observed reported activities as an anti-Tuberculosis agent via multi-linear regression, theoretical compounds were design, carry out simulation screening, predict the ADMET characteristics, and druglikeness of the theoretical inhibitors.

Material and Methods

Dataset generation

Figure 1 and Table 1 are respectively backbone of chemical compound and triazole derivatives. The dataset experimental data were previously reported in the literature [4].

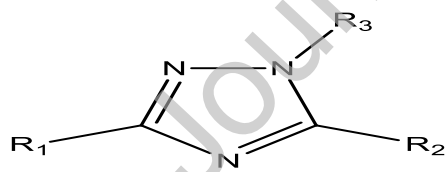


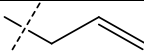
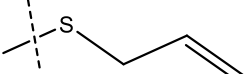
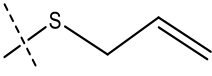
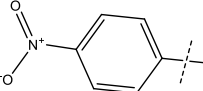
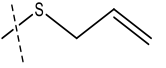

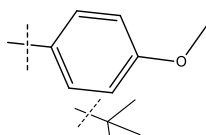
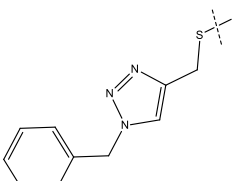
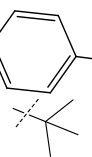
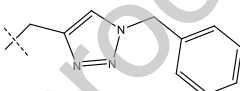
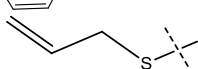
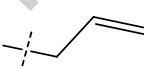
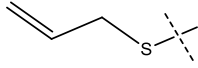
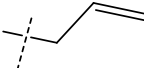
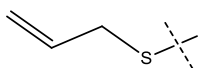
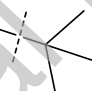
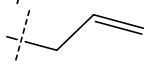
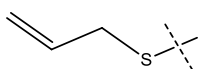
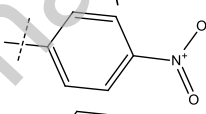
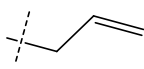
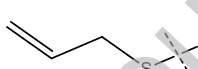
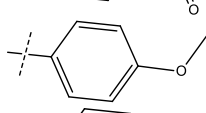
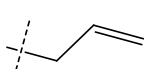

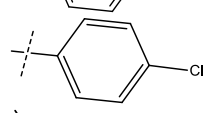
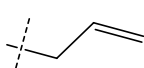
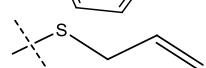
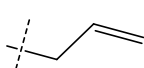
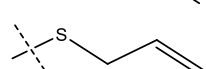
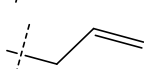
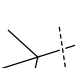
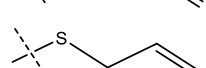
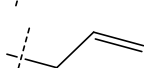
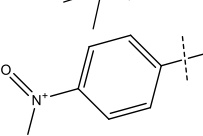
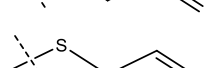
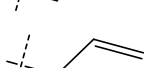


Figure 1: backbone of triazole derivatives

Table 1: Experimental triazole derivatives with their identity

S/ N	R ₁	R ₂	R ₃	Laboratory observed values (pBA)
1 ^a				5.6055

S/ N	R ₁	R ₂	R ₃	Laboratory observed values (pBA)
2				5.381
3 ^a				5.8857
4 ^a				4.8851
5 ^a		H	H	5.6104
6		CH ₃	H	7.9686
7				6.6228
8				6.0461
9 ^a	H			6.25
10	CH ₃			7.2921
11			H	6.6228
12			H	6.8045
13			H	7.4068
14				6.258

S/ N	R ₁	R ₂	R ₃	Laboratory observed values (pBA)
15 a				7.9402
16	CH ₃		H	7.7594
17	CH ₃		H	6.2958
18			H	5.8258
19			H	7.5184
20				5.5163
21		H		6.2768
22		CH ₃		5.6918
23				6.1665
24 a				7.9402
25				7.2447
26				7.5378
27 a	H			7.8219
28 a	CH ₃			7.8546
29 a				5.1504
30				6.1827

S/ N	R ₁	R ₂	R ₃	Laboratory observed values (pBA)
31				7.202
32				5.8884
33 a		H	H	5.4781
34 a			H	4.7861
35			H	6.7355
36		H		7.7243
37		H		7.1866
38		H		7.1927
39		H		6.7506
40		CH ₃		7.8546

Generation of molecular properties

Optimized of all the chemical structures were carried out based on the method previously reported and molecular properties were generated [17].

Data treatment and operation

The data undergo filtration and division into model building set of seventy percent and validation set of thirty percent with the aid of algorithm called Kennard and Stone in order to build mathematical linear regression expression called model that can be used to predict the activity of the hypothetically designed compounds [14].

Development of a model

A bioinformatics software called Material studio, V 8.0 was very instrumental in the building of a mathematical model. The filtered molecular properties were imported into the interphase of the software. Embedded in the material studio is the Genetic function Algorithm with the ability to build several model at a time with their statistical parameters. The best model was chosen based on the statistical parameters, predictive ability and robustness power.

Domain of Applicability (DA)

This domain gives a boundary of ± 3 to the developed *Model* employing the theoretical expression in equation 1. Also in this domain, there were hat matrix (k) to remove unwanted chemical compounds.

$$k_i = M_a(M^R M)^{-1} N_a^T \quad (1)$$

M_a , matrix a with summation of molecular properties. In addition, equation 2 show the theoretical expression for calculating hat matrix [6].

$$k^* = 3 \left(\frac{p+1}{v} \right) \quad (2)$$

p summation of molecular properties in the developed model while, v number of chemical compounds in the model building sets [3, 6].

Randomization test

Y-Randomization evaluation is affirmation approach as previously reported by [3, 19, 20]. The theoretical generated mathematical model emanated by keeping the molecular properties constant while varying the experimental data. For the built model to be ascertain of it quality, that it was not gotten accidentally, R^2 and Q^2 must be very low as previously reported, also, coefficient of Y-randomization must be greater than or equal to 0.5 [3, 20, 21]. Expression three is an equation which must be satisfied for a robust model.

$$cR_p^2 = R \times i[R^2 - (R_r)^2]^{2i} \quad (3)$$

Steps for in-silico screening

After the construction of model, protein target of the inhibitors were downloaded from the protein data bank with an ID code of 3IFZ through resb.org. Figure 2 show the structure of the prepared receptor. The protein was prepared by employing the AutoDock tool embedded in PyRx software as previously reported. [3, 22-24]. To commence the simulation, the x, y, z axes of the binding site grid was set at $50 \times 50 \times 50$ at a spacing of 0.595 \AA . All other simulation procedures followed the approach reported by [22, 25, 26].

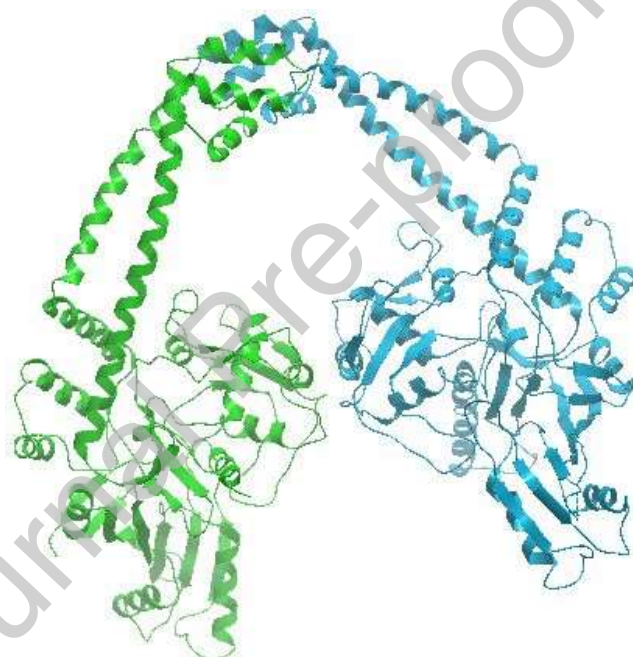


Figure 2. *Crystal structure of DNA gyrase*

Prediction of ADME-Tox and pharmacokinetics assessment

Majority of the drugs fail at the clinical stage due to absent/in-accurate pharmacokinetics predictions. A web-based software called SwissADME was utilized to predict the druggability of the design compounds in order to ascertain their ability as drug candidates, as previously reported in a research carried out [6].

Results*QSAR interpretation studies*

Regression analysis

The model was excellently built using analogues of triazole-1, 2, 4 as a result of their inherent therapeutic ability. Four highly predictive molecular properties with anti-tuberculosis activities as reported in Table 2 while Table 3 show the inborn properties of these molecular properties.

Developed mathematical equation

$$\text{pBA} = -1.2762(\text{MATS7s}) - 2.7874(\text{SM1_DzZ}) - 3.8482(\text{SpMin4_Bhv}) + 0.0207(\text{TDB3v}) + 0.1488(\text{RDF70v}) + 1.5467$$

Table 4 show the statistical parameters and their threshold values of the built model. Also, Y-randomization ($cR_p^2 = 0.8433$) of the developed model.

Table 5 show that validity and potency of the selected molecular properties. Variance Inflation Factor (VIF) is another strong statistical parameters computed for each of the descriptor, as observed in Table 5 [3].

Table 5 is the mean effect (ME) and contribution of each of the molecular properties in the built model.

Figure 3 is a plot of observed activity against predicted activity of the internal validation while Figure 4 is a plot of observed activity versus predicted activity of the external.

Figure 5 shows the residual plot of the activities proposed by the built model. Figure 6 show the William's plot with leverage (k^*)value of 0.64 and a limit of ± 3 .

Table 2. Molecular properties for the dataset

Structure ID	Molecular properties					Theoretical (T) value	Observed (O) value	(T) - (O)	Leverage
	Model building set								
	MAT S7s	SM1_ DzZ	SpMin4_ Bhv	TDB3 v	RDF7 0v				
2	0.0026	1.4821	1.5622	658.7772	2.0498	5.3645	4.3810	0.9835	0.3642
6	0.1182	1.7006	1.3315	746.2645	3.1697	7.7780	7.9686	-0.1906	0.2976
7	0.0516	2.1607	1.7352	685.7303	13.2508	5.1022	5.6228	0.5206	0.4757
8	0.1336	2.5578	1.7289	696.3924	24.0959	5.9593	6.0461	-0.0868	0.1820
10	0.2464	1.9107	1.6606	661.5998	22.5805	7.2229	7.2921	-0.0692	0.1817
11	0.0726	1.9107	1.7655	633.9043	24.8431	6.3599	6.6228	-0.2629	0.1933
12	0.1240	2.5536	1.7727	695.4821	28.0128	6.0378	6.8045	-0.7667	0.1643
13	0.1179	2.1607	1.7717	688.6992	26.4488	7.0721	7.4068	-0.3347	0.1981
14	0.1765	2.5578	1.7713	699.4567	26.6119	6.2889	6.2580	0.0309	0.3157
16	0.0551	1.0536	0.9593	621.0873	0.2906	7.7687	7.7594	0.0093	0.1723
17	0.1773	1.0536	1.1662	572.3149	1.7741	6.4787	6.2958	0.1829	0.2515

Structure ID	Molecular properties					Theoretical (T) value	Observed (O) value	(T) - (O)	Leverage
	Model building set								
	MAT S7s	SM1_ DzZ	SpMin4_ Bhv	TDB3 v	RDF7 0v				
18	0.3859	1.6964	1.4612	732.5999	3.7133	6.4449	5.8258	0.6191	0.1566
19	0.0766	1.3036	1.3745	712.3987	2.8412	7.7195	7.5184	0.2011	0.4540
20	-0.3317	1.9107	1.6962	633.2209	15.5345	5.5578	5.5163	0.0415	0.5045
21	0.0020	1.0536	1.3161	591.6153	1.2108	5.9893	6.2768	-0.2875	0.5295
22	0.1950	1.0536	1.3165	616.2699	2.0915	6.3837	5.6918	0.6919	0.3605
23	-0.2311	1.0536	1.3168	582.2291	2.0369	6.2125	6.1665	0.0460	0.7021
25	0.1290	1.3036	1.4508	688.9992	2.9870	6.8955	7.2447	-0.3492	0.5068
26	0.0164	1.7006	1.3636	712.3814	3.6128	6.8461	6.5378	0.3083	0.3539
30	0.2273	1.6964	1.5063	707.5776	4.1750	6.0236	6.1827	-0.1591	0.3163
31	0.0180	1.3036	1.4669	693.4308	3.4526	7.1364	7.2020	-0.0656	0.6176
32	-0.0601	1.7006	1.3634	717.2290	3.2901	6.9970	5.8884	1.1086	0.1701
35	-0.8213	1.5536	1.2988	621.1500	5.2505	6.9265	6.7355	0.1910	0.2999
36	-0.1353	2.1964	1.3598	773.1185	5.3930	7.1966	7.7243	-0.5277	0.2200
37	-0.2347	1.8036	1.3662	754.5958	5.1746	7.9772	7.1866	0.7906	0.1553

Structure ID	Molecular properties					Theoretical (T) value	Observed (O) value	(T) - (O)	Leverage
	Model building set								
	MAT S7s	SM1_ DzZ	SpMin4_ Bhv	TDB3 v	RDF7 0v				
38	- 0.266 8	2.2006	1.3459	789.7 752	5.088 3	7.7063	7.1927	0.51 36	0.4609
39	0.035 0	1.0536	1.3093	622.7 128	4.643 4	7.1290	6.7506	0.37 84	0.3584
40	0.218 6	1.0536	1.2840	686.1 800	1.051 7	7.7734	7.8546	- 0.08 12	0.7114
			Test set						
1	0.184 1	1.6964	1.4768	703.6 135	4.050 8	6.0916	5.6055	0.48 61	0.2838
3	0.000 8	1.0536	1.3319	584.7 233	4.794 9	6.3206	5.8857	0.43 49	0.2523
4	- 0.167 0	1.4821	1.5640	618.5 815	7.542 5	5.5581	4.8851	0.67 30	0.4252
5	- 0.252 7	1.9107	1.6653	651.0 893	13.78 45	5.6859	5.6104	0.07 55	0.1522
9	- 0.167 3	1.0536	1.2914	619.5 964	1.975 7	6.9944	6.2500	0.74 44	0.4403
15	- 0.002 0	1.0536	1.2318	625.8 344	4.912 7	7.5793	7.9402	- 0.36 09	0.1877
24	- 0.458 1	1.0536	1.2807	634.4 842	1.904 9	7.7049	7.9402	- 0.23 53	0.3766
27	- 0.032 7	1.0536	1.2777	669.1 703	1.282 5	7.8001	7.8219	- 0.02 18	0.1526
28	- 0.138 1	1.0536	1.3086	694.5 662	3.150 3	8.6202	7.8546	0.76 56	0.6140
29	- 0.009 0	0.4286	1.0936	550.5 198	0.357 3	7.6226	5.1504	2.47 22	0.4382

Structure ID	Molecular properties					Theoretical (T) value	Observed (O) value	(T) - (O)	Leverage
Model building set									
	MAT S7s	SM1_ DzZ	SpMin4_ Bhv	TDB3 v	RDF7 0v				
33	- 0.171 8	1.9107	1.6674	657.0 710	14.04 39	5.7372	5.4781	0.25 91	0.2169
34	- 0.332 9	2.5143	1.3369	731.9 698	5.094 70	5.7533	4.7861	0.96 72	0.8236

Residual= (T) - (O)

Table 3: Designation of evolved molecular properties utilized in model building

Identification	Name of molecular properties	Molecular Identity	properties	Dimension
1	Moran-autocorrelation lag-7 / weighted by I-state	MATS7s		2D
2	Spectral moment of order 1 from Barysz matrix / weighted by atomic number	SM1_DzZ		2D
3	Smallest absolute eigenvalue of Burden modified matrix-n 4 / weighted by relative van der Waals volumes	SpMin4_Bhv		2D
4	3D topological distance based autocorrelation - lag 3 / weighted by van der Waals volumes	TDB3v		3D
5	Radial distribution function - 070 / weighted by relative van der Waals volumes	RDF70v		3D

Table 4. Developed model threshold value

S/NO	Validation Parameters	Formula	Threshold	Model
Internal Validation				
1	Friedman Lack of fit (LOF)	$\frac{SEE}{\left(1 - \frac{w + q \times j}{N}\right)^2}$	Significantly low	0.9905
2	R^2	$1 - \frac{\left[\frac{\sum (Y_{obs} - Y_{pred})^2}{\sum (Y_{obs} - \bar{Y}_{training})^2}\right]}{R^2 - P(N - 1)}$	$R^2 > 0.6$	0.7760
3	$adjR^2$	$\frac{N - p + 1}{\left[\frac{\sum (Y_{pred} - Y_{obs})^2}{\sum (Y_{obs} - \bar{Y}_{training})^2}\right]}$	$R^2_{adj} > 0.6$	0.7251
4	Q^2_{cv}	$1 - \frac{\left[\frac{\sum (Y_{pred} - Y_{obs})^2}{\sum (Y_{obs} - \bar{Y}_{training})^2}\right]}{R^2 - P(N - 1)}$	$Q^2 > 0.6$	0.6766
5	Significant Regression			Yes
6	Significance-of-regression F-value			15.25
7	Critical SOR F-value (95%)	$\frac{\sum (Y_{pred} - Y_{obs})^2}{p} / \frac{\sum (Y_{pred} - Y_{obs})^2}{N - p - 1}$	$F_{(test)} > 2.09$	2.6840
8	Replicate points			0
9	Computed observed error			0
10	Min expt. error for non-significant LOF (95%)			0.3763
Model Randomization				
11	Average of the correlation coefficient for randomized data (\bar{R}_r)		$\bar{R} < 0.5$	0.3493
12	Average of determination coefficient for randomized data (\bar{R}_r^2)		$\bar{R}_r^2 < 0.5$	0.1373
13	Average of leave one out cross-validated		$\bar{Q}_r^2 < 0.5$	-0.3038

S/NO	Validation Parameters	Formula	Threshold	Model
14	determination coefficient for randomized data (\bar{Q}_r^2) Coefficient for Y-randomization (cR_p^2)	$R^2 \times \left(1 - \sqrt{ R^2 - \bar{R}_r^2 }\right)$	${}^cR_p^2 > 0.6$	0.8433
External validation				
15	$/r_0^2 - r'^2_0/$		<0.3	0.1638
16	$\frac{r^2 - r_0^2}{r^2}$		<0.1	0.0072
17	$\frac{r^2 - r'^2_0}{r^2}$		<0.1	0.0212
18	R^2_{test}	$R^2_{test} = 1 - \frac{\sum(Y_{pred_{test}} - Y_{obs_{test}})^2}{\sum(Y_{pred_{test}} - \bar{Y}_{training})^2}$	> 0.6	0.6548

Table 5. Statistical assessment of the emanated molecular properties

Molecular properties	MATS7s	SM1_DzZ	SpMin4_Bhv	TDB3v	RDF70v	Mean Effect (ME)	VIF
MATS7s	1					0.0149	1.6291
SM1_DzZ	-0.2249	1				-0.8982	2.7316

SpMin4_Bhv	-0.0384	0.7462	1		-	2.082
					1.083	7
					1	
TDB3v	0.1454	0.5599	0.1767	1	2.725	2.291
					4	5
RDF70v	-0.1903	0.7757	0.08557	0.0598	1	0.251
					0	7

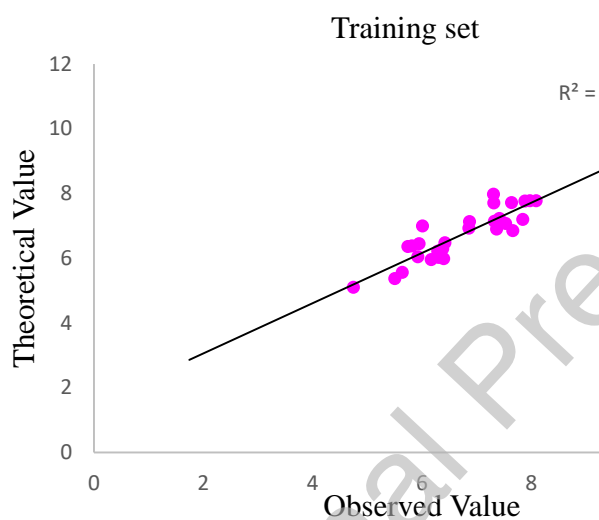


Figure 3. Plot of theoretical value against observed value

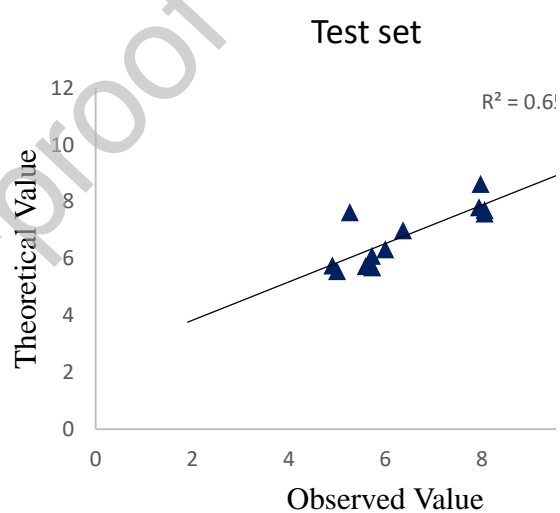


Figure 4. Plot of theoretical value against observed value

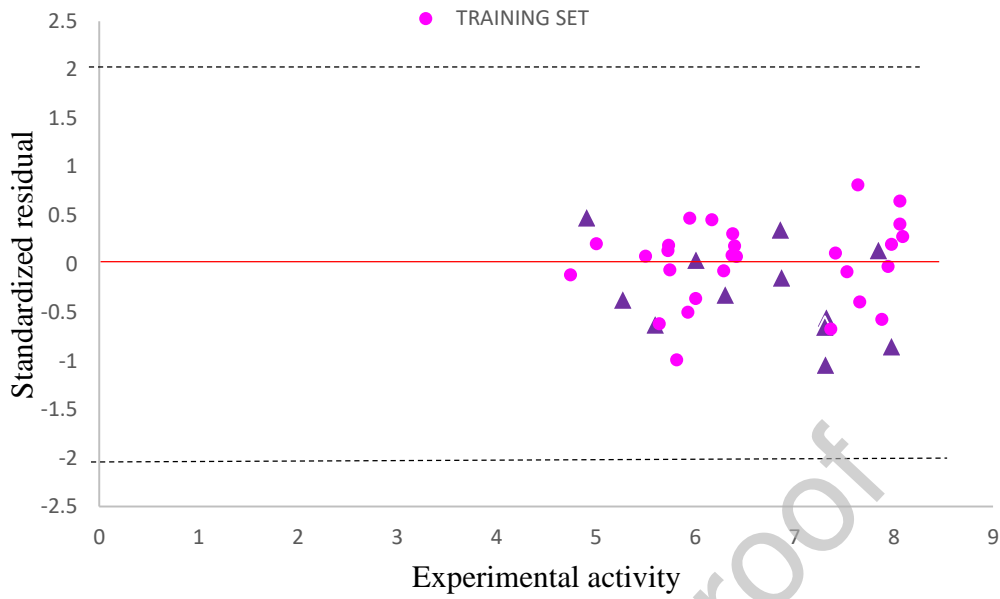


Figure 5. Plot of standardized residual value against observed value.

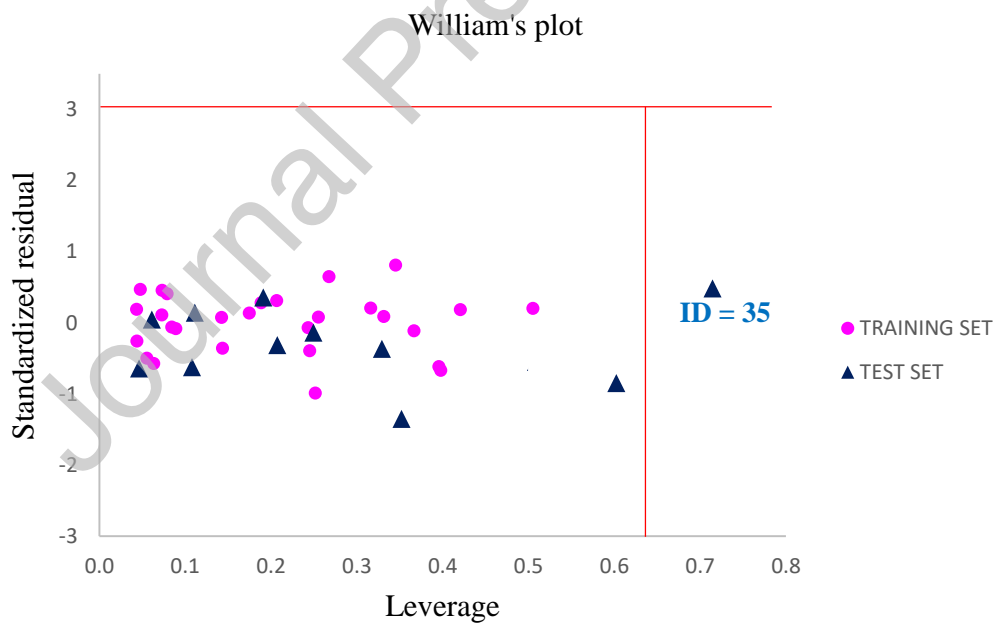


Figure 6. Plot of the standardized residuals vs. the leverage value.

ME analysis is the pivoted point at which the excellent and promising compounds were designed [22]. Figure 7 show the backbone of the structure used in designing new compounds with the highest ME value as shown in Table 5.

Computational design of new anti-tubercular compounds via Ligand-based

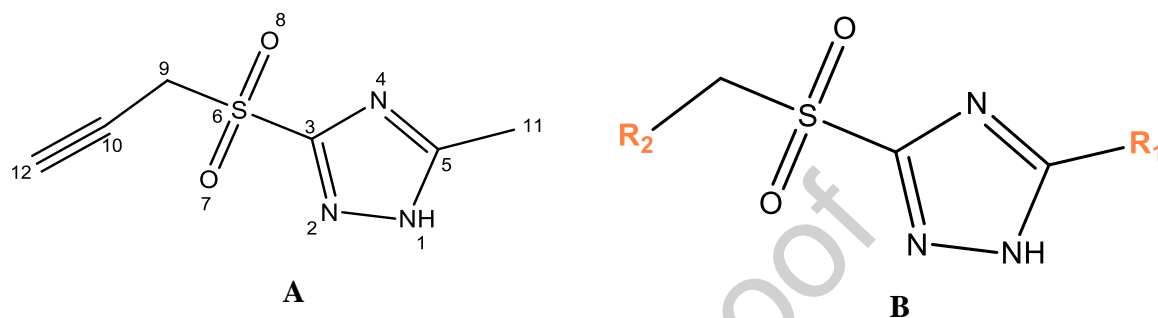


Figure 7: (A) shows the structure of the lead molecule (6). (B) Show the structural template for the lead molecule. Figure 8 show the three theoretical compounds designed after the employment of the template above, namely; x, y, and z. Table 6 show the predicted activities by the proposed model.

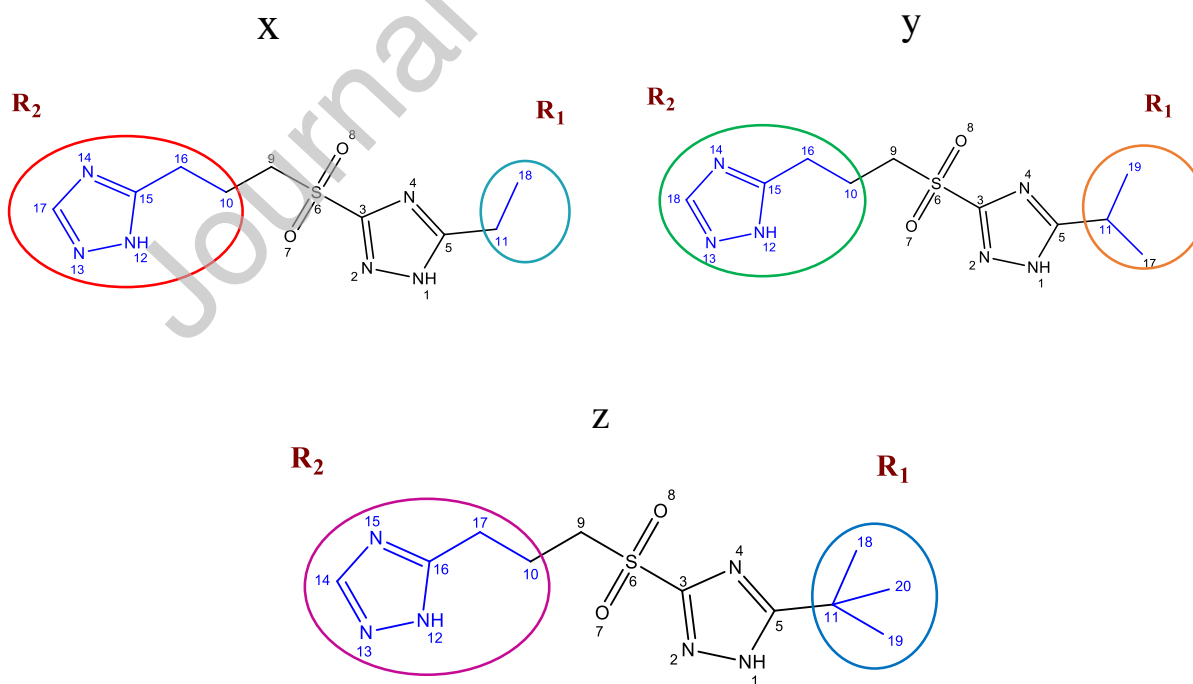
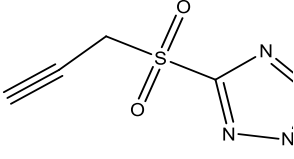
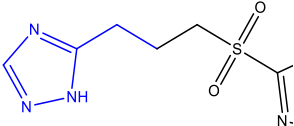
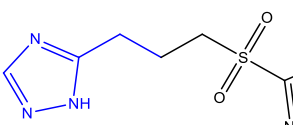
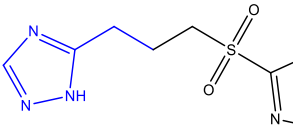


Fig. 8: Chemical structural of the designed compounds x, y and z**Table 6:** Theoretical value of hypothetically designed inhibitors

Identit y	Structure of theoretical inhibitors	Theoretical molecular properties					Theore tical value (pBA)	Lever age
		MAT S7s	SM1_ DzZ	SpMin4 _Bhv	TDB 3v	RDF 70v		
Lead Compound (ID = 6)		- 0.118 2	1.700 6	1.3315	746.2 645	3.16 97	7.9686	0.297 6
x		- 0.124 3	1.529 1	1.2198	628.3 6	13.6 212	8.3136	0.336 2
y		- 0.167 6	1.485 3	1.1946	623.4 5	13.2 016	8.4068	0.284 1
z		- 0.183 3	1.327 1	1.1623	621.5 2	12.2 393	8.7450	0.351 7

Simulation analysis

Table 7 show the docking scores of the theoretically designed inhibitors, x, y, and z with their respective scores of -15.56 kcal/mol, -18.58 kcal/mol, and -18.51 kcal/mol which shows their binding interactions. Figures 9, 10, 11, 12, and 13 show the hydrogen bonds and hydrophobicity of the template and designed inhibitors.

Table 7: Simulation docking interaction

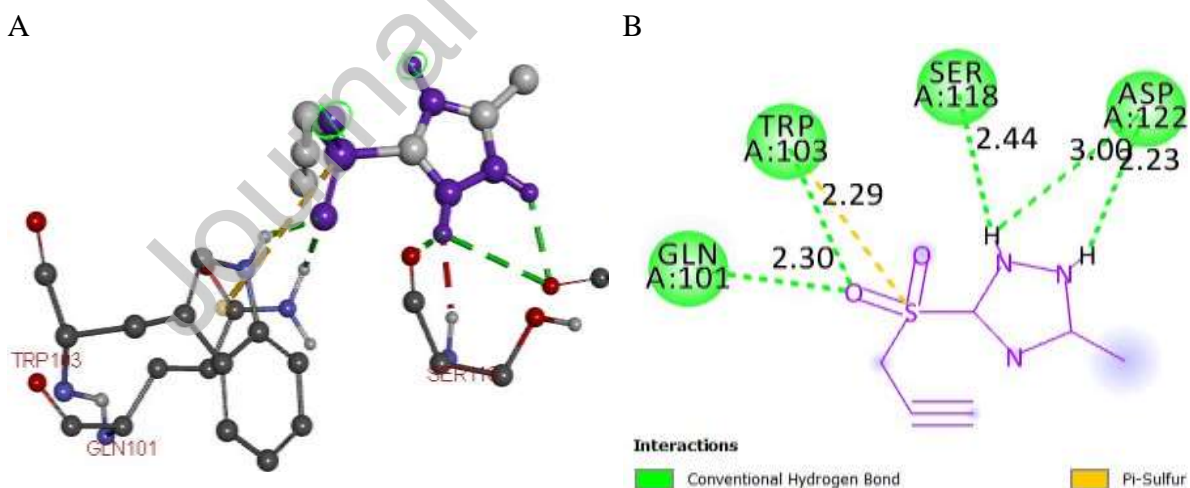
Ligand	CHBI			HI			BA (kcal/mol)	
	AA	CR	BL (Å)	AA	RT	CR		BL (Å)
Lead Compound (ID = 6)	Gln10 1	H- Donor	2.2965	Trp10 3	Pi- Sulfur	Pi- Orbital s	5.2031	-12.41

Ligand	CHBI			HI			BA (kcal/mol)
	AA	CR	BL (Å)	AA	RT	CR	
(Template)	Trp103	H- Donor	2.2855				
	Ser118	H- Acceptor	2.4391				
	Asp12 2	H- Acceptor	2.9977				
	Asp12 2	H- Acceptor	2.2261				
Designed Compound x	Gln10 1	H- Donor	2.5036	Trp10 3	Pi- Sulfur	Pi- Orbitals	5.2182 -15.56
	Trp103	H- Donor	2.1106				
	Ser118	H- Acceptor	2.2327				
	Asp12 2	H- Acceptor	2.1650				
	Pro119	H- Acceptor	2.2034				
Designed Compound y	Val278	H- Acceptor	2.1766				
	Trp103	H- Donor	2.3190	Trp10 3	Pi- Sulfur & Pi-Pi T- shaped	Pi- Orbitals	5.5813 -18.58
	Gly12 0	H- Acceptor	2.3192				

Ligand	CHBI			HI			BA (kcal/mol)
	AA	CR	BL (Å)	AA	RT	CR	
	Gly120	H-Acceptor	2.5560				
	Trp103	H-Acceptor	2.9555				
	Trp103	H-Acceptor	2.4947				
	Pro119	H-Acceptor	2.3494				
	Val278	H-Acceptor	2.7831				
Designed Compound z	Trp103	H-Donor	2.5294	Trp103	Pi-Sulfur & Pi-Pi T-shaped	Pi-Orbitals	5.5033 -18.51
	Gly120	H-Acceptor	2.8383				
	Ser118	H-Acceptor	2.6302				
	Gly120	H-Acceptor	2.1437				
	Pro119	H-Acceptor	2.3107				
	Val278	H-Acceptor	2.8450				

Ligand	CHBI			HI			BA (kcal/mol)
	AA	CR	BL (Å)	AA	RT	CR	
Reference compound (Quinolone)	Trp103	H-Acceptor	2.5764				
	His280	H-Donor	2.6069	Trp103	Pi-Pi T-shaped	Pi-Orbitals	4.8661
	Pro119	H-Acceptor	2.2908	Gln27	Amide -Pi Stacked	Pi-Orbitals	3.9351
	Val278	H-Acceptor	2.6480	Gln27	Amide -Pi Stacked	Pi-Orbitals	4.0396

AA =Amino acid, CR =Chemistry role, BL = Bond length, RT=Reaction type, BA=Binding affinity, HI=Hydrophobic Interaction, CHBI=Conventional Hydrogen Bond Interaction



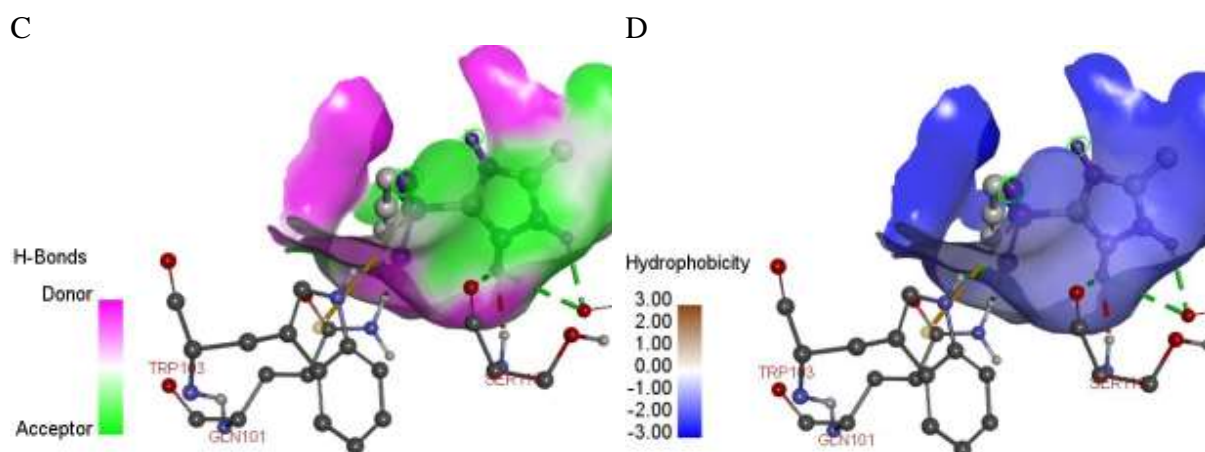


Fig. 9: 3D and 2D view interactions of template compound (compound 6) with the receptor. H-bonding and hydrophobic bonding interactions view of template compound.

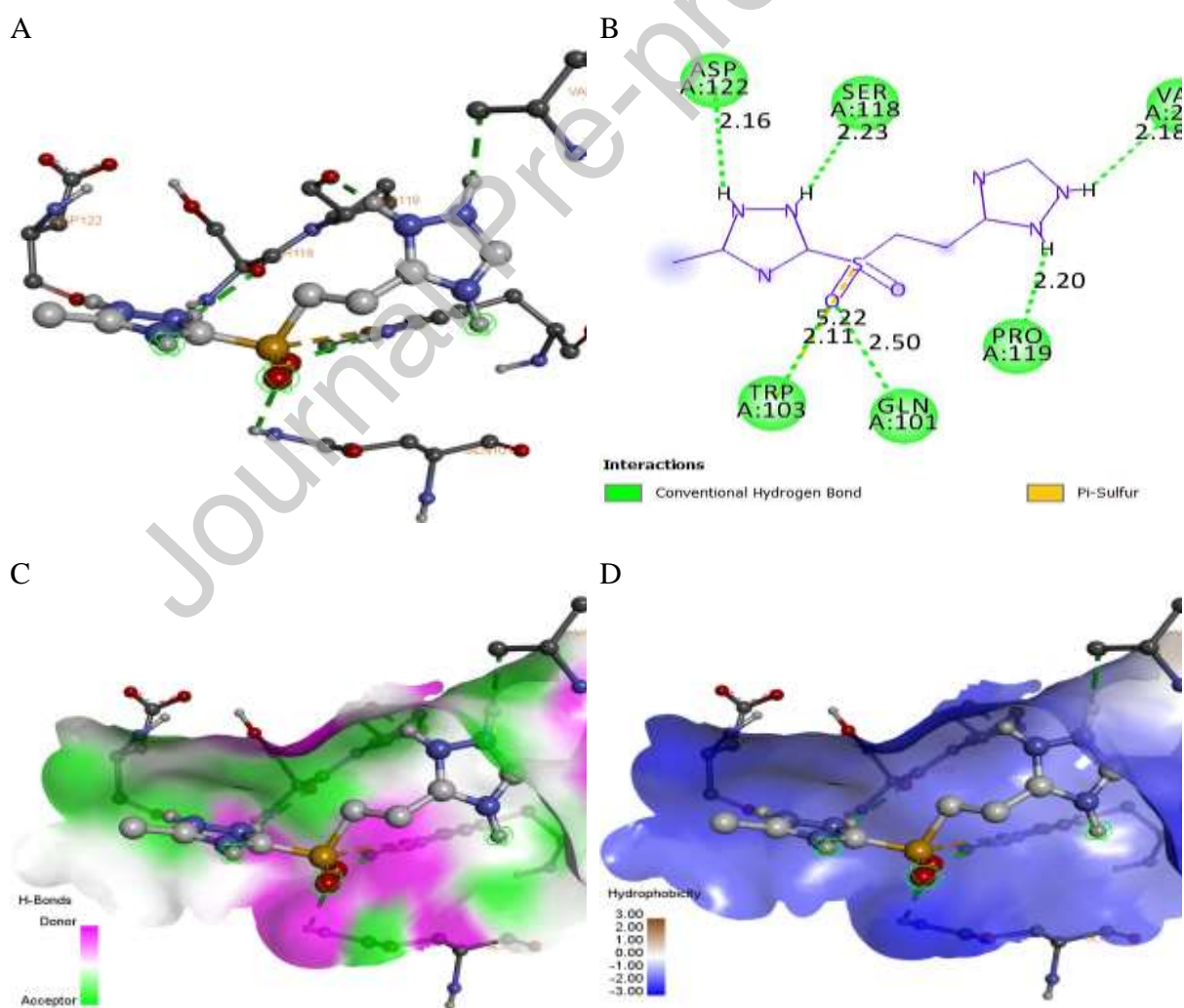


Fig. 10: 3D and 2D view interactions of x compound (theoretical designed) with the receptor. H-bonding and hydrophobic bonding interactions view of x compound.

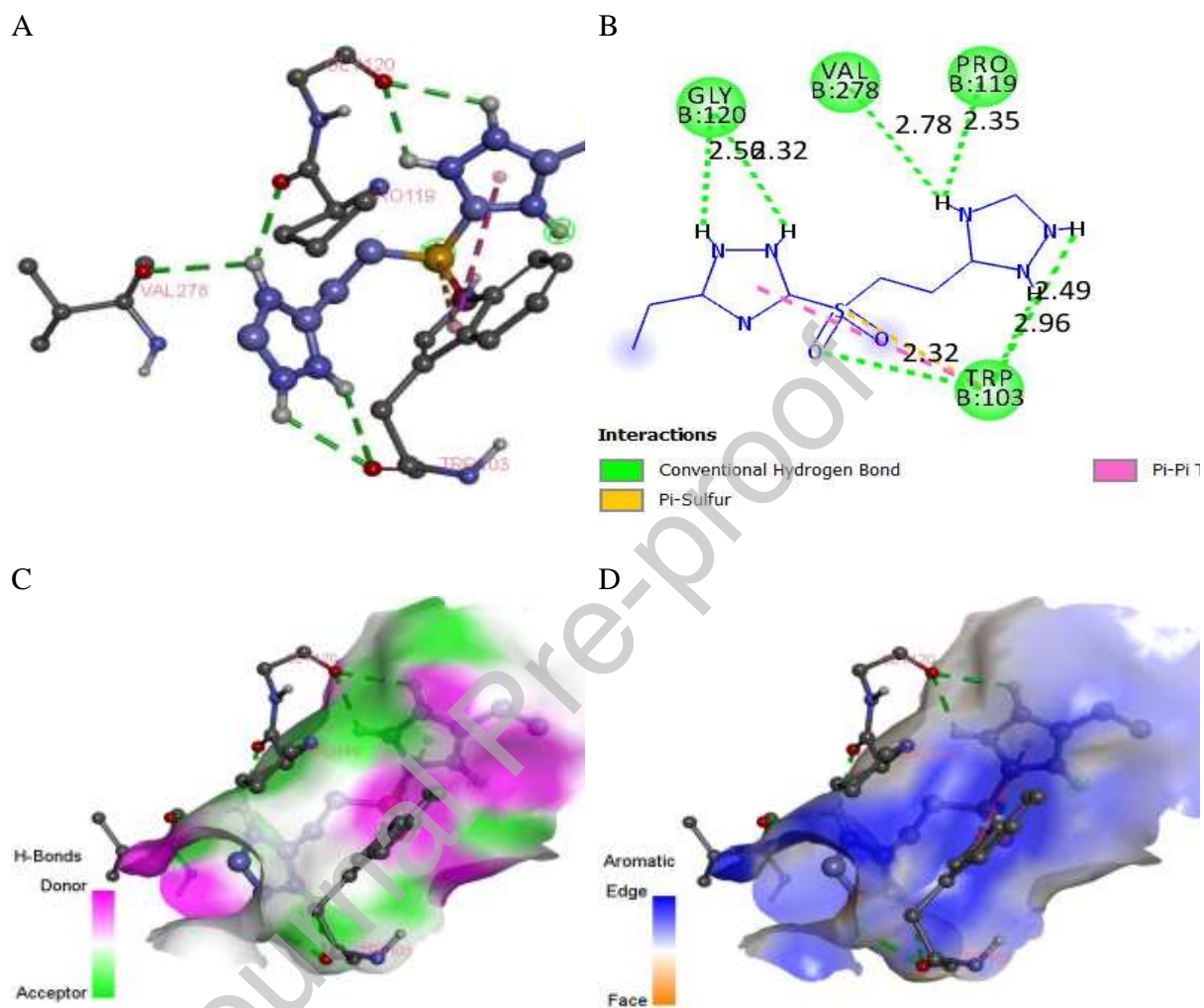


Fig. 11: 3D and 2D view interactions of y compound (theoretical designed) with the receptor. H-bonding and hydrophobic bonding interactions view of y compound.

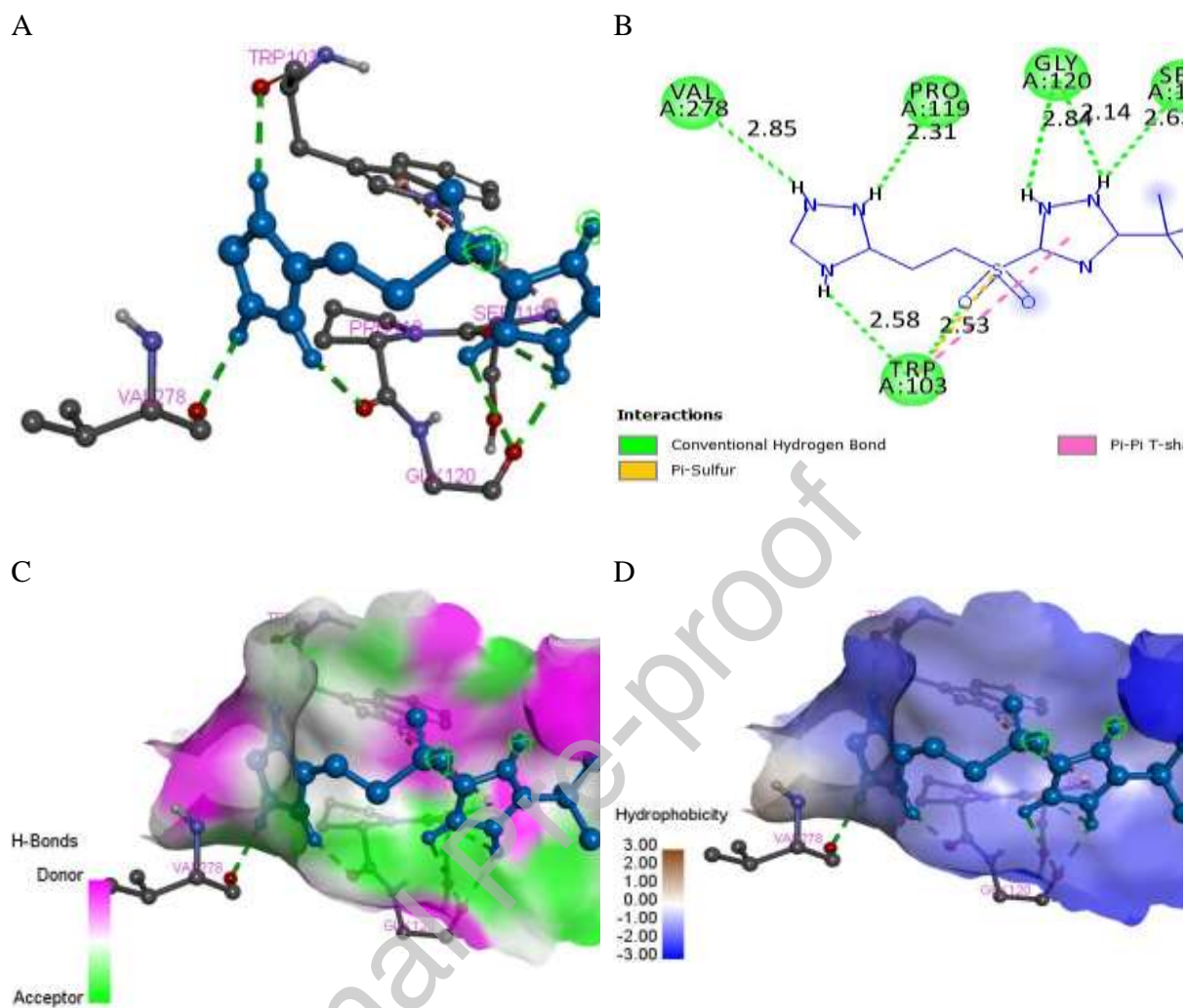


Fig. 12: 3D and 2D view interactions of z compound (theoretical designed) with the receptor. H-bonding and hydrophobic bonding interactions view of z compound.

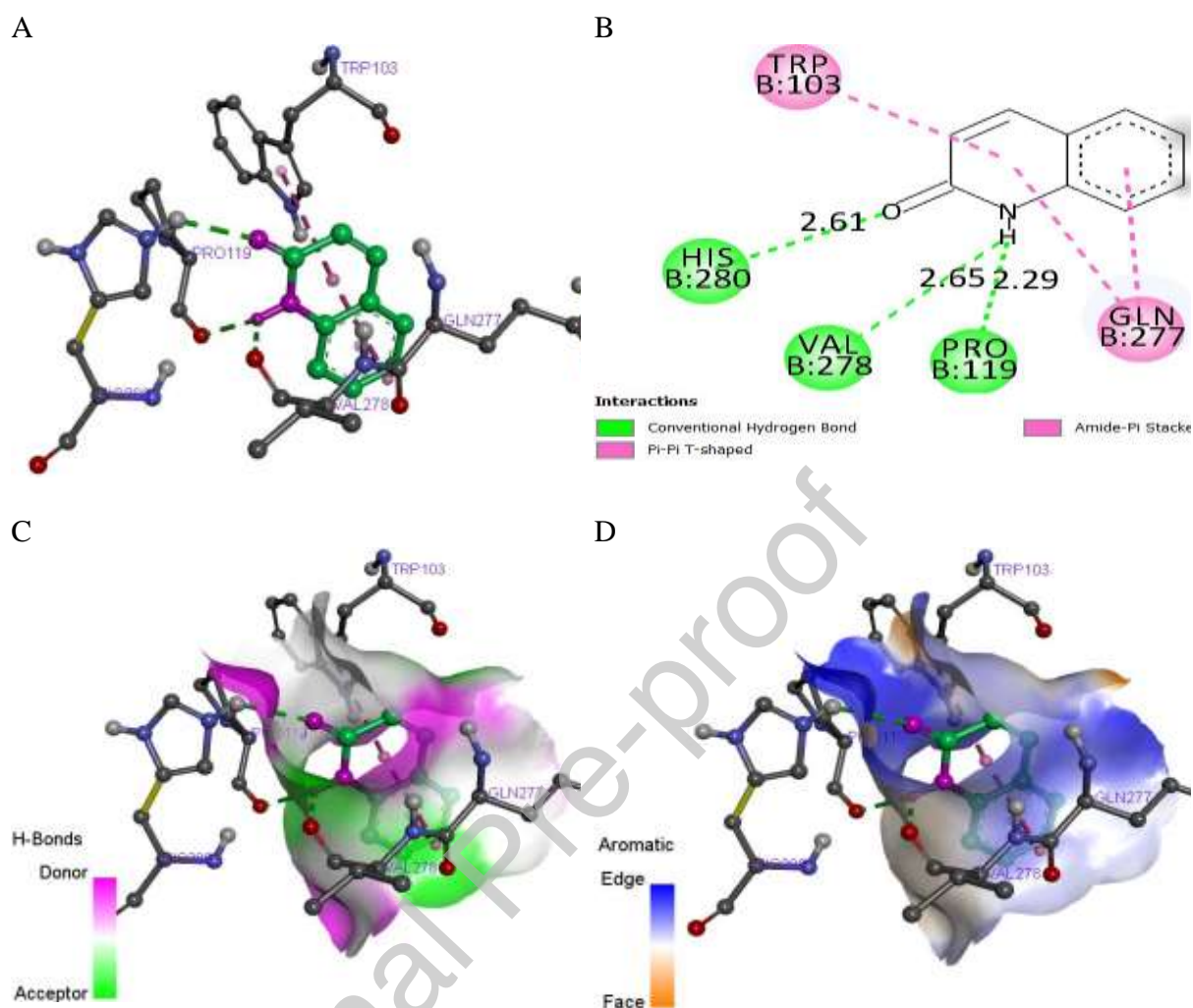


Fig. 13: 3D and 2D view interactions of referenced compound with the receptor. H-bonding and hydrophobic bonding interactions view of referenced compound.

Prediction of ADME-Tox and pharmacokinetics assessment

The Pfizer rule has been utilized to evaluate the drug likeness of potential drug candidates in term of bioavailability. All the Pfizer rule fall within threshold value as shown in Table 8 [28]. The kinetics assessment of designed inhibitors as shown in Table 8. Lastly, still on Table 8, medicinal chemistry parameters (PAINS, Brenk and Leadlikeness) of the designed compounds have their threshold value fall within limit while the template and referenced compounds have their limit outside the threshold value.

Figure 14 show the radar bioavailability of the designed bioactive compounds x, y and z [30].

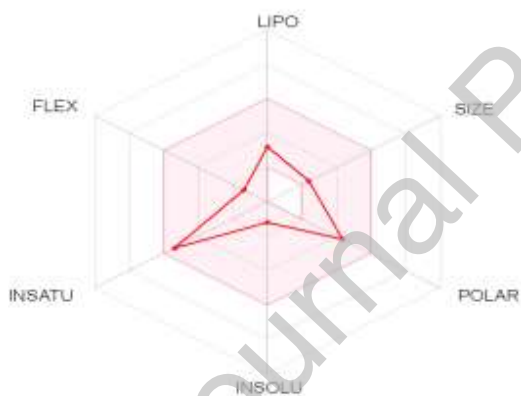
Table 8: Predicted ADME-Tox characteristics and kinetics evaluation

Parameters	Lead	Compound Designed			Reference compound (Quinolone)
	Compound (ID = 6) (Template)	x	y	z	
Descriptors Properties	C ₆ H ₇ N ₃ O ₂ S	C ₉ H ₁₄ N ₆ O ₂ S	C ₁₀ H ₁₆ N ₆ O ₂ S	C ₁₁ H ₁₈ N ₆ O ₂ S	C ₉ H ₇ NO
MW < 500 g/mol	185.20g/mol	270.31g/mol	284.34g/mol	298.36g/mol	145.16g/mol
Num. heavy atoms	12	18	19	20	11
Num. arom. heavy atoms	5	10	10	10	10
Fraction Csp ³	0.33	0.56	0.60	0.64	0.00
Num. rotatable bonds	2	6	6	6	0
nHBA ≤ 10	4	5	6	6	1
nHBD ≤ 5	1	2	2	2	1
Molar Refractivity	42.22	63.29	68.10	72.79	44.57
20 < (TPSA) < 130 Å ²	84.09Å ²	125.66Å ²	125.66Å ²	125.66Å ²	32.86Å ²
Lipophilicity					
iLOGP ≤ 5	0.56	0.31	1.01	0.76	1.56
XLOGP3	0.07	0.80	1.13	1.68	1.26
WLOGP	0.68	0.97	1.53	1.71	1.53
MLOGP	-0.62	-0.92	-0.61	-0.32	1.65
SILICOS-IT	0.69	1.22	1.39	1.59	2.64
Consensus Log Po/w	0.28	0.48	0.89	1.08	1.73
Water Solubility					
Log S (ESOL)	-1.21	-2.04	-2.31	-2.72	-2.21
Solubility	1.15e+01mg/ml ; 6.18e-02mol/l	2.49e+00mg/ml ; 9.22e-03mol/l	1.40e+00mg/ml ; 4.92e-03mol/l	5.66e-01mg/ml ; 1.90e-03mol/l	9.02e-01mg/ml ; 6.22e-03mol/l
Class	Very soluble	Soluble	Soluble	Soluble	Soluble

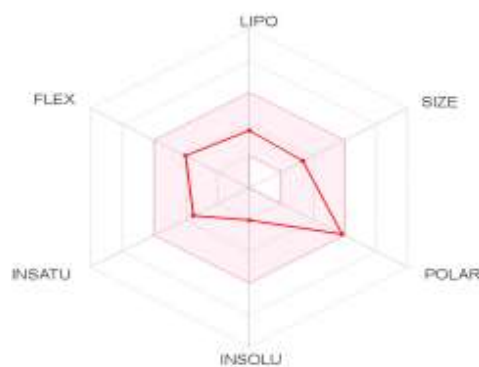
Parameters	Lead	Compound Designed			Reference compound (Quinolone)
	Compound (ID = 6) (Template)	x	y	z	
Log S (Ali)	-1.39	-3.02	-3.36	-3.93	-1.55
Solubility	7.55e+00mg/ml ; 4.08e-02mol/l	2.58e-01mg/ml ; 9.55e-04mol/l	1.23e-01mg/ml ; 4.34e-04mol/l	3.48e-02mg/ml ; 1.17e-04mol/l	4.10e+00mg/ml ; 2.83e-02mol/l
Class	Very soluble	Soluble	Soluble	Soluble	Very soluble
Log S (SILICOS-IT)	-1.66	-3.78	-3.80	-4.19	-3.58
Solubility	4.01e+00mg/ml ; 2.17e-02mol/l	4.51e-02mg/ml ; 1.67e-04mol/l	4.47e-02mg/ml ; 1.57e-04mol/l	1.94e-02mg/ml ; 6.52e-05mol/l	3.78e-02mg/ml ; 2.61e-04mol/l
Class	Soluble	Soluble	Soluble	Soluble	Soluble
Pharmacokinetics					
GI absorption	High	High	High	High	High
BBB permeant	No	No	No	No	Yes
Log Kp (skin permeation)	-7.38cm/s	-7.38cm/s	-7.23cm/s	-6.93cm/s	-6.29cm/s
Druglikeness					
Lipinski	Yes; 0 violation	Yes; 0 violation	Yes; 0 violation	Yes; 0 violation	Yes; 0 violation
Ghose	No; 1 violation: #atoms < 20	Yes	Yes	Yes	No; 2 violations: MW < 160, #atoms < 20
Veber	Yes	Yes	Yes	Yes	Yes
Egan	Yes	Yes	Yes	Yes	Yes
Muegge	No; 1 violation: MW < 200	Yes	Yes	Yes	No; 1 violation: MW < 200
Bioavailability Score	0.55	0.55	0.55	0.55	0.55

Parameters	Lead	Compound Designed			Reference compound (Quinolone)
	Compound (ID = 6) (Template)	x	y	z	
Medicinal Chemistry					
PAINS	0 alert	0 alert	0 alert	0 alert	0 alert
Brenk	1 alert: triple bond	0 alert	0 alert	0 alert	0 alert
Leadlikeness	No; 1 violation: MW < 250	Yes	Yes	Yes	No; 1 violation: MW < 250
Synthetic accessibility	2.67	3.08	3.18	3.29	1.36

MW= Molecular weight, nHBD = number of hydrogen bond donor, nHBA = number hydrogen bond acceptor



Lead compound 6 (Template)



Designed inhibitor x

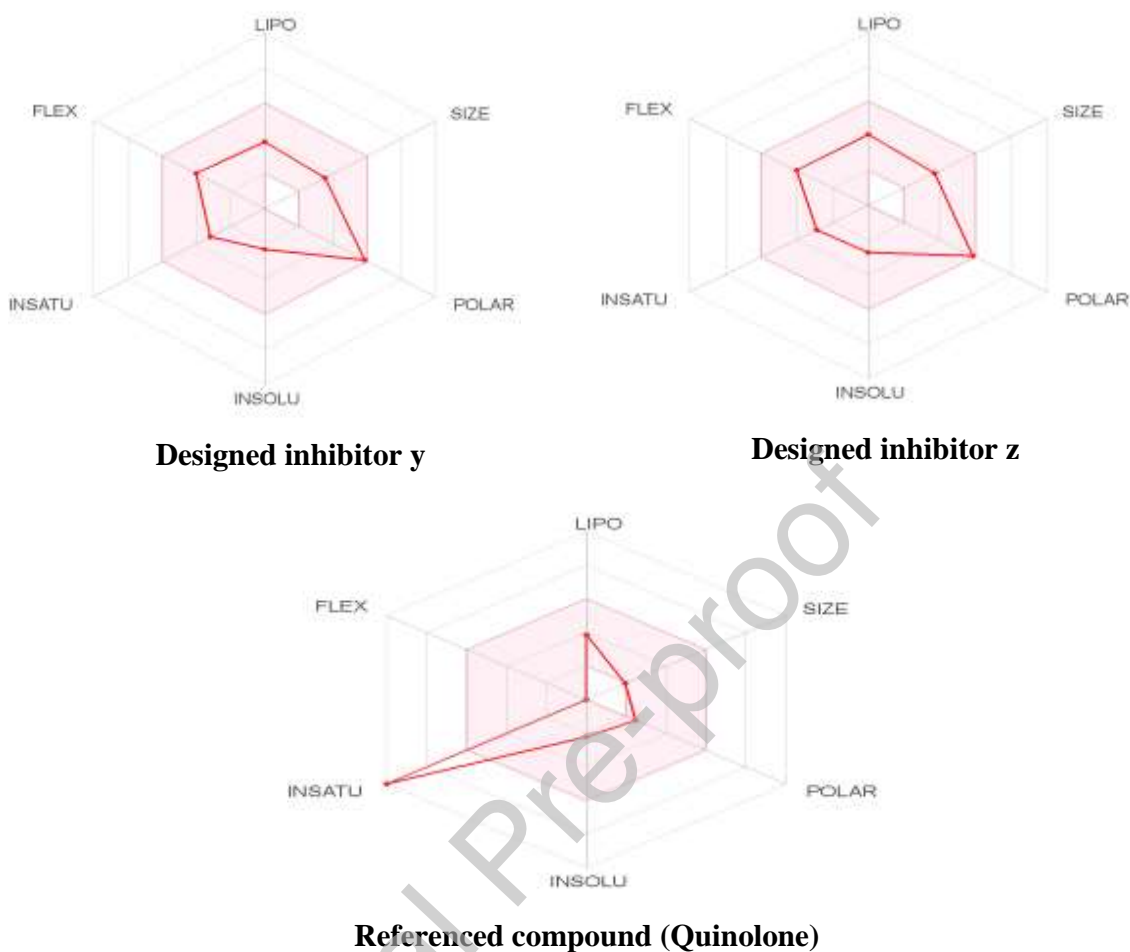


Fig. 14. Radar Bioavailability of the template, designed inhibitors and reference compound

Discussion

QSAR interpretation studies

Regression analysis

The model was excellently built using analogues of triazole-1, 2, 4 as a result of their inherent therapeutic ability. Four highly predictive molecular properties with anti-tuberculosis activities as reported in Table 2 emanated in the model (MATS7s, SM1_DzZ, SpMin4_Bhv, TDB3v and RDF70v). While Table 3 show the inborn properties of these molecular properties. The differences between the predicted and experimental values is the residual values which are very low meaning the model has very significant predictive ability.

Table 4 show the statistical parameters and their threshold values that qualifies robustness of the built model and worth predictive ability for the designed compounds. Also, Y-randomization ($cR_p^2 = 0.8433$) confirmed the sturdy and reliability of the developed model.

Table 5 show that validity and potency of the selected molecular properties were commutated via Person correlation and another statistical test, this fall within threshold value of less than plus or minus 0.8 ($< \pm 0.8$). This means that the properties were excellently good as it appear in the regression model. Variance Inflation Factor (VIF) is another strong statistical parameters computed for each of the descriptor, as observed in Table 5, all the values fall within the limit of VIF less than 10, this implies that the model properties were excellent with good correlation analysis [3]. VIF values above the threshold value implies that the model is not stable and not worth predicting the activities of a designed compounds.

Table 5 is the mean effect (ME) and contribution of each of the molecular properties in the built model. The molecular property TDB3v has the utmost ME attribute of 2.7253, which implies that the descriptor contributed the maximum magnitude to the developed mathematical equation and significantly influence the activities of the designed compounds.

Figure 3 is a plot of observed activity against predicted activity of the internal validation with a correlation value of 0.776 while Figure 4 is a plot of observed activity versus predicted activity of the external validation with a correlation value of 0.6548. These correlation values depicts that the model is good, reliable and sturdy.

Figure 5 shows the residual plot of the activities proposed by the built model. It is obvious that all the values fall within the limit of ± 2 which implies the proposed model have excellent predictions and promising anti-tuberculosis ability.

Figure 6 show the William's plot with leverage (k^*)value of 0.64 and a limit of ± 3 . As it can be observed, compound with ID 35 fall outside the leverage value implies that is an influencer, as such compound ID 35 cannot be consider when designing theoretical compounds.

ME analysis is the pivoted point at which the excellent and promising compounds were designed [22]. Figure 7 show the backbone of the structure used in designing new compounds evolved as a result of the molecular property (TDB3v) with the highest ME value of 2.7253 as shown in Table 5. The significant merit of this molecular property value is that it increase as activity increase and in return it augment the anti-tuberculosis activity, which made TDB3v significant contribution.

Computational design of new anti-tubercular compounds via Ligand-based

Figure 8 show the three theoretical compounds designed after the employment of the template above, namely; x, y, and z. Table 6 show the predicted activities by the proposed model. In order to validate the predicted activities of the designed compounds, the warning leverage (k^*) of 0.64 was compared with calculated leverage generated for the compounds presented in Table 6. All the designed inhibitors fall below the leverage value which confirm the reliability of the predicted activities.

Simulation analysis

Table 7 show the docking scores of the theoretically designed inhibitors, x, y, and z with their respective scores of -15.56 kcal/mol, -18.58 kcal/mol, and -18.51 kcal/mol which shows their binding interactions. These docking scores outweigh that of the referenced compound and the template utilized in the designed of compounds that are respectively -13.22 kcal/mol and -12.41 kcal/mol. Hence, the designed inhibitors exhibited excellent anti-Tuberculosis ability. Detailed simulation analysis results that deeply explains theoretical designed compounds are found in Table 7.

Figures 9, 10, 11, 12, and 13 show the hydrogen bonds and hydrophobicity of the template which has five hydrogen bonds in the complex and two amino acids viz; Gln101 and Trp103, compound x has six hydrogen bonds in the complex with two amino acids viz; Gln101 and Trp103, compound y has a sum of seven hydrogen bonds in the complex with one amino acid, viz; Trp103, compound z has a sum of seven hydrogen bonds in the complex with one amino acid viz, Trp103, and the referenced compound has a total of three hydrogen bonds interactions in the complex respectively.

It could be infer from the above analysis that the three designed compounds have six and seven hydrogen bonds with the same amino acid interaction. This conspicuous observation emanate from the modification point in the template as shown in Figure 7 which enhanced their binding poses with efficient binding interactions with the target receptor.

Prediction of ADME-Tox and pharmacokinetics assessment

The Pfizer rule has been utilized to evaluate the drug likeness of potential drug candidates in term of bioavailability. All the Pfizer rule fall within threshold value as shown in Table 8. This implies that three designed inhibitors are orally active and has been proved in a previous research [28]. The physicochemical properties such as MW, HBA, HBD, TPSA of the designed compounds exhibited small polarization and elasticity as a result of their forecasted TPSA fall within the limit. The merit of this is that the theoretically designed compounds are excellently admirable.

The lipophilicity which is basically water and octanol ratio of all the designed compounds fall within threshold limit which means that, in lipid environment, the compounds are very good and druggability. The water solubility of compounds x, y, and z with all the solubility values fall within the expected limit, the compounds are soluble and worth inspecting for drug evaluation and used as drug candidates. The kinetics assessment of designed inhibitors as shown in Table 8, could be useful because they penetrate human intestinal absorption and blood brain barrier. Also, these compounds have their permeant ability less than -2.5 cm/s, it implies that the compounds can penetrate the skin. Keen inspection of Table 8, it will be observed that properties such as Egan, Ghose, Mueggae, ans Veber which fall under drug-likeness have no violation and all their score values are 'YES' unlike the referenced compound with two violation that is 'NO' under Ghose and Mueggae rules, this suggest that the three designed compounds are excellent drug candidates compared to the referenced compound.

Lastly, still on Table 8, medicinal chemistry parameters (PAINS, Brenk and Leadlikeness) of the designed compounds have their threshold value fall within limit while the template and referenced compounds have their limit outside the threshold value. Hence, all the three designed compounds have good medicinal Chemistry properties.

Figure 14 show the radar bioavailability of the designed bioactive compounds x, y and z. The physicochemical area is depicted by pink for a bioavailable chemical compound as previously reported in a research [30]. Keenly inspection of Figure 14 show that all the three designed compounds fall within the orally pink bioactive region which the compounds are medically bioactive compare to the referenced compounds that have a point outside the pink region and simply mean non-bioactive.

Journal Pre-proof

Conclusion

Computational-Aided Drug Design have been successfully carried out on forty (40) triazole 1,2,4 derivatives in building a model with outstanding molecular properties (MATS7s, SpMin4_Bhv, SM1_DzZ, TDB3v and RDF70v) with anti-tuberculosis curing ability. Simulation techniques were employed for virtual screening and designing of inhibitors. After the molecular docking, compound six (6) emanated as a template because of its lowest docking score, it was then used as a template to design several compounds out of which three compounds; x (-15.56 kcal/mol), y (-18.58 kcal/mol), and z (-18.51 kcal/mol) emanated as the best with docking scores lower than the template and the referenced compound. Lastly, these designed compounds were subjected to ADMET-ox prediction and pharmacokinetics assessment, all the compounds successfully passed the evaluation and fit-well as potential drug candidates. This research has immensely contributed in the 2063 African agenda to cure any life threatening disease. The compounds can be subjected to further clinical test such as *in-vitro* and *in-vivo* analysis.

ABBREVIATION

Not applicable in this section

REFERENCES

- [1] W.H.O (2019) <http://www.who.int/news-room/fact-sheets/detail/tuberculosis>
- [2] W.H.O (2021) https://www.who.int/health-topics/tuberculosis#tab=tab_1
- [3] Ajala, A., Uzairu, A., Shallangwa, G. A., & Abechi, S. E. (2022). 2D QSAR, design, docking study and ADMET of some N-aryl derivatives concerning inhibitory activity against Alzheimer disease. *Future Journal of Pharmaceutical Sciences*, 8(1), 30. <https://doi.org/10.1186/s43094-022-00420-w>
- [4] <https://patents.google.com/patent/US9376402B2/en>

- [5] P.S. Abideen, K. Chandrasekaran, V.A. Maheswaran, V. Kalaiselvan, Implementation of self-reporting pharmacovigilance in anti-tubercular therapy using knowledge based approach. *Journal of Pharmacovigilance*, 23 (2013) 20-34. <https://doi.org/10.4172/2329-6887.1000101>
- [6] Ajala, A., Uzairu, A., Shallangwa, G. A., & Abechi, S. E. (2022). Structure-based drug design of novel piperazine containing hydrazone derivatives as potent Alzheimer inhibitors: molecular docking and drug kinetics evaluation. *Brain Disorders*, 7, 100041. <https://doi.org/10.1016/j.dscb.2022.100041>
- [7] C. W. James, DNA entanglement and the action of the DNA Topoisomerases, Cold Spring Harbor Laboratory Press, Cold Spring Harbor, NY. (2009). 245.
- [8] Y.Y. Huang, J.Y. Deng, J. Gu, Z.P. Zhang, A. Maxwell, L.J. Bi, Y.Y. Chen, Y.F. Zhou, Z.N. Yu, X.E. Zhang, The key DNA-binding residues in the Cterminal domain of Mycobacterium tuberculosis DNA gyrase A subunit (GyrA). *Nucleic Acids Reseach*, 34 (2006) 5650–5659. <https://doi.org/10.1093/nar/gkl695>
- [9] Y. Zhang, K. Post-Martens, S. Denkin, New drug candidates and therapeutic targets for tuberculosis therapy. *Drug Discovery Today*, 11 (2006) 21-27. [https://doi.org/10.1016/S1359-6446\(05\)03626-3](https://doi.org/10.1016/S1359-6446(05)03626-3)
- [10] B.S. Holla, M. Mahalinga, M.S. Karthikeyen, B. Poojary, P.M. Akberali, N.S. Kumari, Synthesis, characterization and anti-microbial activity of some substituted 1, 2, 3-triazoles. *European Journal of Medical Chemistry*, 40 (2005) 1173-1178. <https://doi.org/10.1016/j.ejmech.2005.02.013>
- [11] H.N. Hafez, H.A. Abbas, A.R. El-Gazzar, Synthesis and evaluation of analgesic, anti-inflammatory and ulcerogenic activities of some triazolo- and 2- pyrazolylpyrido[2,3-d]- pyrimidines. *Acta Pharmacy*, 58 (2008) 359-378. <https://doi.org/10.2478/v10007-008-0024-1>
- [12] L.P. Guan, Q.H. Jin, G.R. Tian, K.Y. Chai, Z.S. Quan, Synthesis of some quinoline-2 (1H)-one and 1, 2, 4-triazolo[4, 3 -a] quinoline derivatives as potent anticonvulsants. *Journal of Pharmacy and Science*, 10 (2007) 254-262. <https://doi.org/10.1021/jm801343r>
- [13] R. Gujjar, A. Marwaha, J. White, L. White, S. Creason, D.M. Shackelford, J. Baldwin, W.N. Charman, Identification of a metabolically stable triazolopyrimidine-based dihydroorotate dehydrogenase inhibitor with activity in mice. *Journal of Medicinal Chemistry*, 52 (2009) 1864-1872. <https://doi.org/10.1021/jm801343r>

- [14] Abduljelil, A., Uzairu, A., Shallangwa, G. A., & Abechi, S. E. (2023). Virtual screening, molecular docking simulation and ADMET prediction of some selected natural products as potential inhibitors of NLRP3 inflammasomes as drug candidates for Alzheimer disease. *Biocatalysis and Agricultural Biotechnology*, 102615. <https://doi.org/10.1016/j.bcab.2023.102615>
- [15] Y.S. Mary, P.B. Miniyar, Y.S. Mary, K.S. Resmi, C.Y. Panicker, S. Armaković, S.J. Armaković, R. Thomas, B. Sureshkumar, Synthesis and spectroscopic study of three new oxadiazole derivatives with detailed computational evaluation of their reactivity and pharmaceutical potential, *Journal of Molecular Structure* (2018), : 10.1016/j.molstruc.2018.07.026.
- [16] S. Beegum, Y.S. Mary, Y.S. Mary, R. Thomas, S. Armakovic, S.J. Armakovic, J. Zitko, M. Dolezal, C. Van Alsenoy, Exploring the detailed spectroscopic characteristics, chemical and biological activity of two cyanopyrazine-2-carboxamide derivatives using experimental and theoretical tools, *Spectrochimica Acta Part A: Molecular and Biomolecular Spectroscopy*, 224 (2020) 117414 <https://doi.org/10.1016/j.saa.2019.117414>
- [17] Ajala, A., Uzairu, A., Shallangwa, G. A., & Abechi, S. E. (2023). QSAR, simulation techniques, and ADMET/pharmacokinetics assessment of a set of compounds that target MAO-B as anti-Alzheimer agent. *Future Journal of Pharmaceutical Sciences*, 9(1), 1-20.. <https://doi.org/10.1186/s43094-022-00452-2>
- [18] Ajala, A., Uzairu, A., Shallangwa, G. A., & Abechi, S. E. (2022). Computational and pharmacokinetics studies of 1, 3-dimethylbenzimidazolinone analogues of new proposed agent against Alzheimer's disease. *Beni-Suef University Journal of Basic and Applied Sciences*, 11(1), 1-19.. <https://doi.org/10.1186/s43088-022-00231-1>
- [19] K. Roy, P. Chakraborty, I. Mitra, P.K. Ojha, S. Kar, R.N. Das, Some case studies on application of “rm2” metrics for judging quality of quantitative structure–activity relationship predictions: emphasis on scaling of response data, *J. Comput. Chem.* 34 (2013) 1071–1082. QSAR models-strategies and importance, *Int. J. Drug Des. Discov.* 3 (2011) 511–519. <https://doi.org/10.1002/jcc.23231>
- [20] Ajala, A., Uzairu, A., Shallangwa, G. A., & Stephen, A. E. (2022). QSAR, Molecular Docking, Dynamic Simulation and Kinetic Study of Monoamine Oxidase B Inhibitors as

- Anti-Alzheimer Agent. *Chemistry Africa*, 1-14. <https://doi.org/10.1007/s42250-022-00561-8>
- [21] A. Tropsha, P. Gramatica, V.K. Gombar, The importance of being earnest: validation is the absolute essential for successful application and interpretation of QSPR models, *Mol. Inform.* 22 (2003) 69–77. <https://doi.org/10.1002/qsar.200390007>
- [22] Ajala, A., Uzairu, A., & Suleiman, I. O. (2016). Chemometric study of some α , β -unsaturated ketone as potential antifungal agents using density function theory and GFA (ATCC 10231 and NCIM 3446 cell line). *Cogent Chemistry*, 2(1), 1175073. <https://doi.org/10.1080/23312009.2016.1175073>
- [23] J. Piton, S. Petrella, M. Delarue, G. Andre´-Leroux, V. Jarlier, A. Aubry, C. Mayer, Structural Insights into the Quinolone Resistance Mechanism of Mycobacterium tuberculosis DNA Gyrase, *PLoS ONE* 5 (2010), e12245. doi:10.1371/journal.pone.0012245.
- [24] <https://www.rcsb.org/structure/3IFZ>
- [25] O. Adedirin, A. Uzairu, G. A. Shallangwa, S. E. Abechi, A novel QSAR model for designing, evaluating, and predicting the anti-MES activity of new 1H-pyrazole-5-carboxylic acid derivatives. *Journal of the Turkish Chemical Society*, 4 (2017). 739–774. <https://doi.org/10.18596/jotcsa.304584>
- [26] M.T Ibrahim, A Uzairu, G.A Shallangwa, S Uba, In-silico activity prediction and docking studies of some 2, 9-disubstituted 8-phenylthio/ phenylsulfinyl-9 h-purine derivatives as Anti-proliferative agents. *Heliyon* 6(2020) e03158. <https://doi.org/10.1016/j.heliyon.2020.e03158>
- [27] N.B. Patel, I.H. Khan, S.D. Rajani, Pharmacological evaluation and characterizations of newly synthesized 1,2,4-triazoles. *European Journal of Medicinal Chemistry*. 45 (2010). <https://doi.org/10.1016/j.ejmech.2010.06.031>
- [28] C. A. Lipinski, Rule of five in 2015 and beyond: Target and ligand structural limitations, ligand chemistry structure and drug discovery project decisions. *Advanced Drug Delivery Reviews*, 101 (2016) 34–41. <https://doi.org/10.1016/j.addr.2016.04.029>
- [29] R. Mannhold, G. I. Poda, C. Ostermann, I.V. Tetko, Calculation of molecular lipophilicity: State-of-the-art and comparison of log P methods on more than 96,000 compounds. *Journal of Pharmaceutical Sciences*, 98 (2009). 861–893. <https://doi.org/10.1002/jps.21494>
- [30] A. Daina, O. Michielin, V. Zoete, SwissADME: A free web tool to evaluate pharmacokinetics,

drug-likeness and medicinal chemistry friendliness of small molecules. *Scientific Reports*, 7 (2017). 1–13. <https://doi.org/10.1038/srep42717>

Credit Author Statement

Stephen E. Abechi, Ajala Abduljelil, Abatyough Terungwa Michael and Otaru Habiba Asipita, and Mohamed El Fadil did the conception and design of the work. **Stephen E. Abechi, Ajala Abduljelil, Abatyough Terungwa Michael and Otaru Habiba** the acquisition and analysis of the data. **Stephen E. Abechi, Ajala Abdulelil, Abatyough Terungwa Michael and Otaru Habiba** interpreted the data. **Ajala Abduljelil** drafted the manuscript. **Ajala Abduljelil** substantively revised the manuscript. All authors read and approved the final manuscript

Declarations

Ethics approval and consent to participate

Not applicable

Consent for publication

Not applicable

Availability of data and Materials

Not applicable

Funding

Not applicable

Acknowledgements

The authors gratefully acknowledged the technical effort of Dr. Abdulfatai Usman, Mr Stephen Ejeh and Dr Samuel Adawara all of chemistry department, Ahmadu Bello University, Zaria.

Declaration-of-competing-interests

The authors declare that they have no competing interests

Journal Pre-proof